CROATICA CHEMICA ACTA
CCACAA **80** (3-4) 493–502 (2007)
ISSN-0011-1643
CCA-3192
Original Scientific Paper

Formation and Stabilization of Noble Metal Nanoparticles*

Szilvia Papp,[a] Rita Patakfalvi,[a] and Imre Dékány[a,b,]**

[a]*Nanostructured Materials Research Group of the Hungarian Academy of Sciences, H-6720 Szeged, Hungary*

[b]*Department of Colloid Chemistry University of Szeged, Aradi Vértanúk tere 1, H-6720 Szeged, Hungary*

RECEIVED DECEMBER 6, 2006; REVISED FEBRUARY 15, 2007; ACCEPTED FEBRUARY 19, 2007

The kinetics of homogeneous and heterogeneous nucleation processes of metal (Ag, Pd) nanoparticles was studied by UV-VIS spectrometry. Silver nanoparticles were prepared in aqueous solution by homogeneous nucleation using poly(vinylpyrrolidone) (PVP) and sodium citrate as sterical stabilizers. Reduction was ensured by adding hydroquinone. According to kinetic functions, reduction is an autocatalytic process: a slow, continuous nucleation is followed by a fast, autocatalytic growth. The presence of polymer inhibits nucleation and retards the rate of particle growth. Formation of palladium nanoparticles was investigated in aqueous medium *via* reduction by hydrazine, using PVP and the clay mineral hectorite as stabilizers. Effects of the polymer and concentration of silicate and palladium ions on the particle formation rate were analyzed. The rate of reduction is decreased by increasing amounts of stabilizing agents and increased by increasing concentrations of precursor ions. The kinetics of heterogeneous nucleation was determined based on the adsorption of the palladium species at the clay mineral particles and the viscosity of the hectorite dispersion.

Keywords
palladium
silver
nanoparticle formation
UV-VIS spectroscopy
TEM

INTRODUCTION

Modern microscopes developed in the last few decades have revolutionized the development of nanotechnological research. Scientists have recognized that the physical and mechanical properties of nanosize particles differ from those of macroscopic material. The preparation and characterization of precious metal nanoparticles of outstanding practical importance have come into the focus of cutting-edge research.

Various methods are available for their preparation. It is essential that aggregation be prevented in the course of preparation; in this way, the synthesis of even very small particles (in the size range of a few nanometers) becomes possible. The most widely used techniques make use of physical limitations of the preparation environment, like in reactions staged inside inverse micelles,[1,2] porous solid materials,[3] gels,[4] polymers[5] or dendrimers.[6] John Bradley classified reactions that have so far been utilized for the preparation of transition metal particles into four groups corresponding to four types of methods.[7] Due to its simplicity and effectivity, the currently most preferred preparation method is liquid phase reduction of metal salts. The reducing agent employed is mainly hydrogen gas,[8,9] hydrazine[10,11] or sodium borohydride,[12,13] but citrate,[14,15] hypophosphorous acid[16] and oxidizable solvents such as alcohols[17,18] have also been successfully used in synthetic reactions.

---

* Dedicated to Professor Nikola Kallay on the occasion of his 65th birthday.

** Author to whom correspondence should be addressed. (E-mail: i.dekany@chem.u-szeged.hu)

Few publications address the kinetics of nanoparticle formation. According to a mechanism proposed by Watzky and Fink at the end of the nineteen-nineties, slow continuous nucleation followed by fast autocatalytic surface growth results in nearly monodisperse size distribution.[19] It has been experimentally proven that stronger reducing agents promote the formation of nuclei with smaller diameters, which then continue to grow.[20] Growth may proceed in two different ways. According to one conception, nuclei formed in the first stage join together, whereas another theory proposes that already solidified particles are further enlarged by collisions with freshly reduced metal ions. The notion accepted in special literature is that the final size is determined by the relative rates of nucleation and growth. This notion is the basis of the most efficient method of nanoparticle synthesis presently known, *i.e.,* »controlled colloidal synthesis« (CCS), which allows arbitrary variation of particle size by varying the ratio of the rate of nucleation to that of particle growth.

The kinetics of particle formation can be followed in a variety of experimental setups. UV-VIS spectroscopy is applied to the characterization of metal and semiconductor nanoparticles with plasmon resonance lines in the visible range. Henglein monitored the stepwise growth of silver clusters by spectroscopic methods.[21] According to his results, growth follows an autocatalytic reaction pathway that includes adsorption of metal ions and their subsequent reduction on the surface of the zero-valent metal cluster.

Caia *et al.*[22] studied the formation of silver nanoparticles stabilized by hexanethiol as revealed by their UV-VIS absorbance spectra. The characteristic absorption peak of silver was first shifted towards lower wavelengths and later, as the reaction progressed, towards higher wavelengths. It was deduced from these observations that in the first part of the reaction large particles were formed, which later fell apart to give rise to smaller ones, and later also those started to grow. The reaction could be described by a first-order rate equation.

Hoogsteen and Fokkink prepared polymer-stabilized Pd hydrosols, using hypophosphorous acid (H_3PO_2) as reductant.[16] The presence of polyvinyl alcohol (PVA), a compound weakly adsorbing to the surface of palladium, had no effect on the kinetics of particle formation, and particle size was not controllable either. However, polyvinyl pyrrolidone (PVP), a polymer strongly binding to metal surfaces, did affect the kinetics of particle formation and particle size: in its presence, smaller particles were formed. Poly-2-vinyl pyrrolidone (P2VP) affects the process of sol formation not only by its high affinity to metal surfaces, but also, by virtue of its cationic character, through complex formation with the precursor salt $PdCl_4^{2-}$. These authors also established that particle size decreases with increasing the concentrations of the stabilizing polymer and the reducing agent. Ayyappan later made similar observations on other metal sols.[23] Busser and coworkers studied the strength of the coordination between rhodium ions and various polymers.[24] They found that precursor ions cannot be reduced when the interaction is too strong, whereas a weak coordination leads to the formation of large particles. It was observed in the course of photochemical preparation of silver nanoparticles stabilized by PVP[25] that higher PVP concentrations bring about a faster photochemical reaction: Ag particles interact with excited C=O* groups, which reduce Ag^+ ions to metallic silver.

Esumi *et al.* prepared Pd organosols stabilized by polyvinyl pyrrolidone (PVP) from various precursor molecules by ethanol reduction.[26] The size distribution of particles generated by reduction of $Pd(OAc)_2$ was nearly monodisperse (2–4 nm), whereas slow reduction of $Pd(OAc)_2$ resulted in the formation of particles with a relatively wide size distribution. Increasing the amount of polymer added was found to decrease size. Kim *et al*. selected various silver salts and studied the effect of the chemical nature of the precursor on the formation rate of metal nanoparticles.[27] In the presence of $AgBF_4$, $AgPF_6$ and $AgClO_4$, the fast initial reaction rate slowed down after about 10 min whereas in the case of $AgNO_3$, a slower but constant reaction rate was observed. They attributed this phenomenon to the strong interaction between silver and nitrate ions. The course of the absorbance spectra also allows conclusions to be drawn as to the size, size distribution and the aggregation state of nanoparticles.[28–30]

Seregina *et al.* synthesized Au, Pd, Pt and Rh nanoparticles by block copolymers.[31] Their studies on the effect of several reducing agents showed that hydrazine hydrate reduced precursor ions much slower than did $NaBH_4$ whereas phenyl hydrazine only complexed but failed to reduce them. Ingelstein and coworkers prepared platinum nanoparticles in w/o microemulsions by borohydride reduction of H_2PtCl_6. The organic phase was n-heptane and the stabilizers used were alcohol ethoxylates and AOT. They studied the effect of surfactant type on the kinetics.[32] Particles smaller than the droplet size of the microemulsion (5 nm) were obtained in all cases. In their experience, droplet fusion is facilitated when the surfactant is more readily solubilized in the oil phase. In this case, the rate is determined by droplet fusion whereas in other cases the reducing agent has an influence on the rate as well.

In the work described here, we studied the formation of silver and palladium nanoparticles in homogeneous phase and on the surface of supports. Our aim was to study the effects of metal ion and reducing agent concentrations and of the presence of polymers on the ratio of the rates of nucleation and nucleus growth by spectrophotometrically monitoring the formation of polymer-stabilized sols in aqueous media. In addition, we also investigated the kinetics of heterogeneous nucleation in the course of the synthesis of palladium particles in optically transparent hectorite suspensions.

MATERIALS AND METHODS

Materials

Precursors: $AgNO_3$ (Reanal, 99.9 %), $PdCl_2$ (Aldrich, 99 %)

Reducing agents: ethanol (C_2H_5OH, *p.a.*, Reanal), hydroquinone (Aldrich, 99 %), hydrazine hydrate ($NH_2NH_2 \cdot H_2O$, 24–26 % (mass fraction, *w*) aqueous solution, Fluka)

Stabilizing agents: sodium citrate dihydrate (Aldrich, 99 %), polyvinyl pyrrolidone (PVP, $M_w = 40000$, Fluka)

Supports: magnesium silicate (optigel SH, $Si_8O_{20}(OH)_4Mg_{5.33}Li_{0.67}$, Süd Chemie, $a^S = 350 \pm 50$ m^2/g)

Methods

UV-VIS Absorption Spectroscopy. – UV-VIS absorption studies were performed in an Uvikon 930 dual-beam spectrophotometer. Measurements were made in 1 cm quartz cuvettes in the wavelength range of 200–800 nm. Adsorption of nanoparticles on clay minerals was followed by measuring the spectrum of the supernatant. Kinetics of nanoparticle formation was studied in an Ocean Optics Chem 2000-UV-VIS diode array spectrophotometer equipped with fiber optics in the wavelength range of 200–800 nm. Sols were prepared in the cuvette of the instrument. Starting from the moment of the reductant addition, the spectrophotometer automatically stored the spectra at pre-programmed intervals. In the course of reduction, the reaction mixture was stirred using a micromagnetic stirrer.

Transmission Electron Microscopy (TEM). – Size analysis of metal nanoparticles was carried out using a Philips CM-10 electron microscope (acceleration voltage 100 kV) equipped with a Megaview-II digital camera. Solid samples were studied in dilute aqueous suspensions while in the case of sols, droplets of the undiluted material were placed on Formwar-coated copper mesh grids (diameter 2 mm). The average particle diameter and size distribution of the samples were determined by the UTHSCSA Image Tool 2.00 software, based on the data of an average of 200 particles. The maximal resolution of the microscope is *ca*. 0.2 nm.

RESULTS AND DISCUSSION

The Kinetics of Particle Formation

Kinetic Analysis of the Formation of Palladium Nanoparticles. – Homogeneous nucleation of palladium particles was studied without stabilizer or in the presence of PVP. 3.9 cm^3 of 0.5 % (mass concentration, ρ) PVP was added to a quartz cuvette (path length 1 cm), followed by the addition of 50 μL of 3 mmol dm^{-3} $PdCl_2$ in hydrochloric acid and, under constant magnetic stirring, by the injection of 50 μL of hydrazine solution (pH = 3.8). The reference solution was a polymer solution of appropriate concentration. Changes in the spectrum of the system prepared in this way (total volume 4 cm^3) were recorded by the diode array detector every 1–2 s for 10 min.

For studies of heterogeneous nucleation, polymer molecules were replaced with a Mg-silicate variety that forms an optically transparent suspension (hectorite, Optigel SH) as stabilizer. Since the aqueous suspension of commercial Optigel SH is highly alkaline (pH = 10–11), it was treated with 1 mol dm^{-3} hydrochloric acid for 24 h, washed with distilled water to pH = 7.5, centrifuged, dried at room temperature and ground. The solid support obtained in this way was swollen in water before use. Volumes added were identical with those described for homogeneous nucleation. The experiments involved variation of the concentrations of suspensions (0.01–0.5 % (ρ)) and precursor ions (0.019–0.075 mmol dm^{-3}).

Formation of Palladium Particles by Homogeneous Nucleation in Polymer Solution. – The spectrum of the aqueous palladium chloride solution used for the kinetic experiments (pH = 3.6) displays a peak at 212 nm and a shoulder at 237 nm (Figure 1). According to the literature data, these are characteristic of $[PdCl_3(H_2O)]^-$ and $[PdCl_2(H_2O)_2]$ complexes.[33] The references in our experiments were polymer solutions.

Figure 1 shows temporal changes in the spectrum of palladium ions reduced without stabilizer. The reaction is completed instantaneously and later the spectrum shows hardly any change. Absorbance at wavelengths above 250 nm is significantly increased, indicating the formation of relatively large palladium particles/aggregates.

A set of curves with values decreasing with increasing wavelengths was recorded in the course of reduction. Since there is no peak characteristic of palladium nanoparticles, their formation can be monitored by following the decrease in precursor ion concentration or the in-

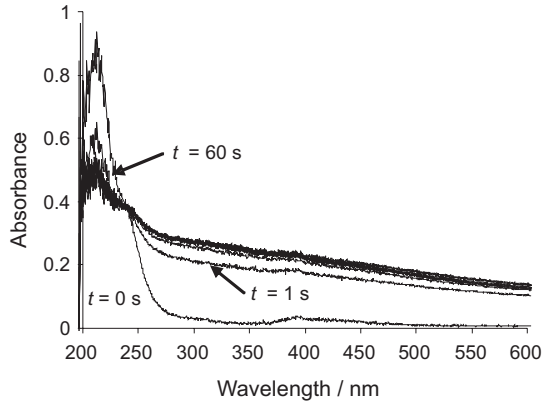

Figure 1. Reduction of $PdCl_2$ solution (without stabilizer) followed up by UV-VIS spectroscopy.

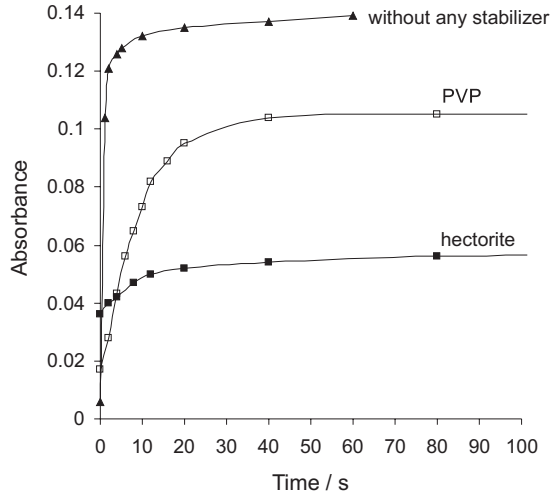

Figure 2. Absorbance (λ = 600 nm) *vs.* time curves of Pd nanoparticles stabilized by hectorite and PVP ($c_{stabilizer}$ = 0.5 % (ρ) and $c_{Pd^{2+}}$ = 0.038 mmol dm^{-3}).

crease in absorbance at higher wavelengths. The increase in absorbance indicates an increase in the number and size of the particles formed. Because of the noise at the maximum, we chose the latter method. Accordingly, we characterized particle formation by the increase in absorbance values measured at λ = 600 nm.

Kinetic curves do not allow differentiation of nucleation and nucleus growth. We characterized the rate of the process as a whole by the slope of the initial section of the absorbance *versus* time function, which we term apparent kinetic constant (k^*). In the case of reduction without stabilizer, the apparent kinetic constant of particle formation is k^* = 0.098 s^{-1}.

Experience shows that the slope of straight lines obtained by linearization of UV-VIS absorption spectra decreases with increasing particle size. By fitting a power function to the data reported for Pt sols by Furlong, the possible sizes of particles formed in systems of various compositions were determined based on the relationship obtained (d /nm = 5.574 · $S^{1.017}$ where S is the slope).[34] Absorbance values of the spectra were normalized to λ = 450 nm and, after plotting the lgλ – lg$A$ function, S of the above equation was replaced by the slope of the straight line obtained. Slopes and the corresponding particle diameters are listed in Tables together with compositions of the systems (Table I). The results show that, 60 s after reduction, the size of particles formed in the absence of stabilizer is 7.3 nm. TEM images show 6–20 nm aggregates consisting of individual particles with an average diameter of $d_{ave.}$ = 2.1 nm.

When using PVP as stabilizer, the spectrum displayed in Figure 3 is obtained. It is clearly seen in Figure 2 that the initial rate is much lower than that of reduction without stabilizer. Absorbance does not increase after 40 s (A = 0.104) and remains below the value measured without stabilizer (A = 0.137). Average particle diameter calculated from the spectrum is 3.8 nm. This means that the PVP molecule is capable of binding strongly to the metal surface and inhibiting growth by collision.

Formation of Palladium Particles by Heterogeneous Nucleation in Mg-silicate Suspensions. – The kinetics of particle formation was also studied on the surface of synthetic hectorite (Mg-silicate). In part of the experiments the concentration of Pd^{2+} ions was kept constant ($c_{0,Pd^{2+}}$ = 0.075 mmol dm^{-3}) and hectorite concentration was varied in the range of 0.5–0.001 % (ρ). When $PdCl_2$ solution was added to the hectorite suspension, the measured pH was 5.8.

Hectorite slows down reduction more than polymers do (Figure 2), most probably because structure formation by the lamellae obstructs free flow of the reducing agent by increasing viscosity.

We provided experimental proof that increasing the concentration of the suspension results in an increase in

TABLE I. Composition of prepared systems, kinetic parameters and particle diameters

Stabilizer	Stabilizer conc. / % (ρ)	$c_{0,Pd^{2+}}$ / mmol dm^{-3}	Pd content / % (w)	Pd content / mmol g^{-1}	k^* / s^{-1}	$\tau_{1/2}$ / s	$S^{(a)}$	d / nm
–	–	0.075	–	–	0.098	7.07	0.77	7.3
PVP	0.5	0.075	_	–	0.0065	106.64	1.46	3.8
hectorite	0.5	0.075	0.16	0.015	0.0013	533.19	2.80	2.0
	0.1	0.075	0.79	0.075	0.0059	117.48	2.54	2.2
	0.02	0.075	3.84	0.375	0.0102	67.95	2.00	2.8
	0.02	0.056	2.89	0.280	0.0075	92.42	2.57	2.1
	0.02	0.038	1.98	0.190	0.0048	144.41	2.23	2.5
	0.02	0.019	1.00	0.095	0.0028	247.55	1.84	3.0
	0.001	0.075	44.39	7.500	0.022	31.51	1.61	3.4

[(a)] S = –d lg A / d lg λ, where A is the absorbance value measured at λ nm

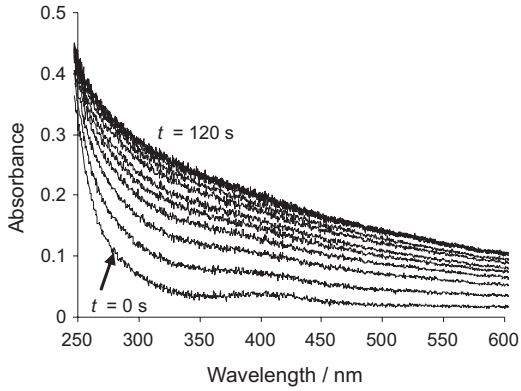

Figure 3. Formation of Pd nanoparticles stabilized with PVP followed up by UV-VIS spectroscopy.

viscosity (results not shown). Thus, reduction may have become diffusion-inhibited due to the presence of hectorite lamellae. In addition to increased viscosity, another factor greatly contributing to deceleration is the fact that the majority of Pd^{2+} species are adsorbed on the surface. Adsorption of Pd^{2+} ions on hectorite was tested in a separate experiment. All the ions were bound to the surface in the concentration range studied, which means that nucleation takes place on the surface.

At a hectorite concentration of 0.001 % (ρ) the spectrum changes as shown in Figure 4. The reaction rate increases with decreasing hectorite concentration; the apparent rate constants determined are listed in Table I, and the *A vs. t* functions are summarized in Figure 5a. The apparent rate constant (k^*) is considerably increased ($0.0013\ s^{-1} \rightarrow 0.022\ s^{-1}$) due to the 500-fold dilution. The calculated particle size increases with decreasing hectorite concentration. This is not surprising considering the significant change in palladium content normalized to hectorite mass (see Table).

We studied the rate-determining role of precursor ions in a hectorite suspension with constant concentration of 0.02 % (ρ) (Figure 5b). The concentration of the

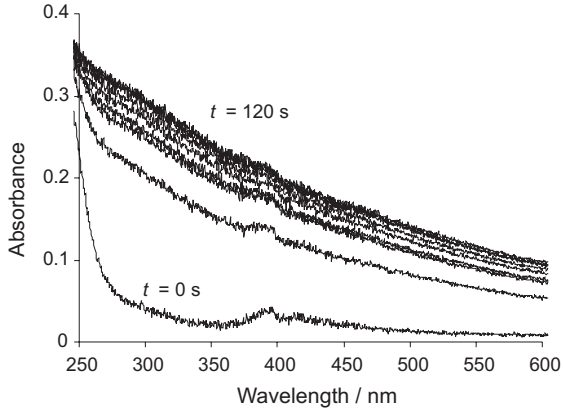

Figure 4. Formation of Pd nanoparticles on hectorite surface followed up by UV-VIS spectroscopy ($c_{hectorite}$ = 0.001 % (ρ), $c_{Pd^{2+}}$ = 0.075 mmol dm^{-3}).

$PdCl_2$ solution was varied between 0.019 and 0.075 mmol dm^{-3}. The initial slope of the *A vs. t* functions decreased with decreasing concentration, indicating deceleration of reduction. Half-life increases considerably ($67.95\ s^{-1} \rightarrow 247.5\ s^{-1}$) (Table I). Particle size first decreases, then increases, which may also mean aggregation of the primary particles. These data suggest that there is an optimal concentration range where nucleation rate is maximal, and this is where the smallest particle size can be attained. At higher concentrations, the particle diameter increases due to the supply of material; on the other hand, a decrease in concentration may slow the process to such an extent that particle growth is favored.

We attempted to determine, by TEM, the size of the particles formed in the course of experiments. Due to the shielding effect of hectorite, only the image of the sample with the lowest hectorite concentration could be eva-

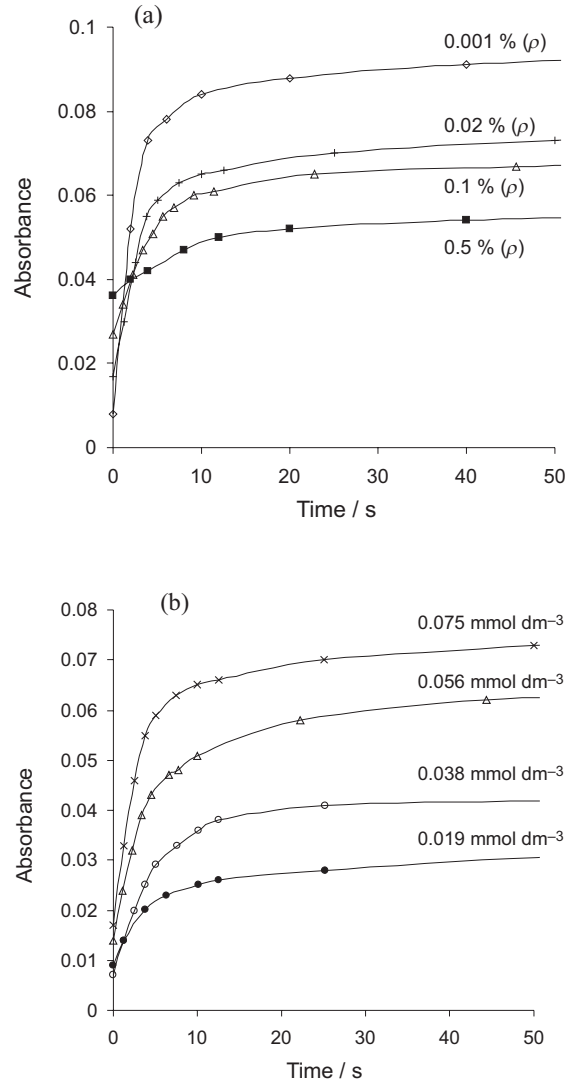

Figure 5. Absorbance (λ = 600 nm) *vs.* time curves of Pd nanoparticles stabilized by hectorite (a) at constant Pd^{2+} ion and varying hectorite concentrations, and (b) at constant hectorite and varying Pd^{2+} ion concentrations.

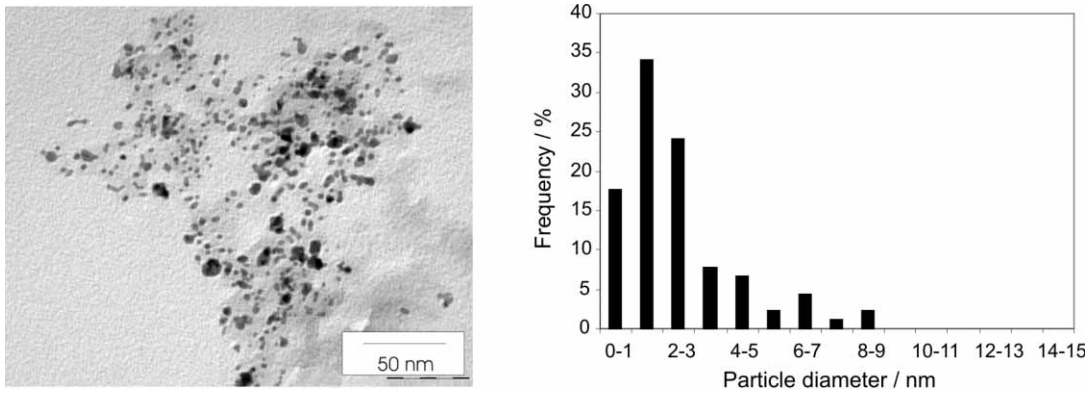

Figure 6. TEM micrograph of Pd nanoparticles prepared on hectorite lamellae ($c_{hectorite}$ = 0.001 % (ρ) and $c_{Pd^{2+}}$ = 0.075 mmol dm^{-3}, $d_{ave.}$ = 2.8 nm).

luated. The image of the hectorite/palladium composite made at 180,000× magnification (Figure 6) displays partially aggregated particles.

Preparation of Silver Particles in Polymer Solution. – All components, with the exception of the reductant, were added to a 1 cm quartz cuvette (in a total volume of 2.8 cm^3: the necessary amount of 0.5 mol dm^{-3} aqueous polymer solution was made up to 1.0 cm^3 with distilled water, 1.2 cm^3 of 10 mmol dm^{-3} Na-citrate solution and 0.4 cm^3 of 10 mmol dm^{-3} $AgNO_3$ solution). From the moment of adding the reductant (0.2 cm^3 of 1 mmol dm^{-3} aqueous hydroquinone solution), absorption spectra were recorded every minute for 40 minutes at room temperature. In the course of reduction, the reaction mixture was stirred with a micromagnetic stirrer.

Kinetic Analysis of the Homogeneous Nucleation of Silver Nanoparticles. – Hydroquinone is one of the relatively milder reductants used for the reduction of silver ions. At appropriately selected hydroquinone concentrations, the rate of particle formation and thereby the size of the generated particles can be controlled. We used Na-citrate and PVP to slow the reaction and to act as stabilizer.

Absorption spectra of an Ag sol containing 0.07 g/100 cm^3 PVP, recorded every minute for 20 min, are shown in Figure 7. The initial phase of the reaction is very fast; after about 20 min, particle formation slows down. At a PVP concentration of 0.07 g/100 cm^3, maximal absorbance measured after 20 min exceeds 1.5. The wavelength of the maximum of the silver absorption band (λ = 420 nm) is not altered in the course of the reaction.

Figure 8 reveals that the absorbance maxima of PVP-stabilized sols always fall short of the value measured in the polymer-free sol. It can be also observed that the spectra of Ag sols prepared in PVP solutions are less symmetrical. The spectrum of the sol prepared in 0.5 g/100 cm^3 PVP displays a shoulder in the higher wavelength range, indicating the presence of larger, aggregated particles.[25] Polymer molecules join individual particles into larger aggregates.

For a kinetic characterization of particle formation, absorbances measured at 420 nm were plotted against time at several polymer concentrations (Figure 9). The course of the functions reveals that a slow induction process takes place first, and later the process is accelerated. In the case of PVP, the process can be considered as complete in about 25 min for each sol, since absorbance remains nearly constant. We assume that the first, relatively slow stage corresponds to nucleation, which does not bring about any considerable increase in absorbance. After 5–8 minutes, the faster process already involves nucleus growth. This assumption is also in accord with the effect of polymer concentration. It is clear that, due

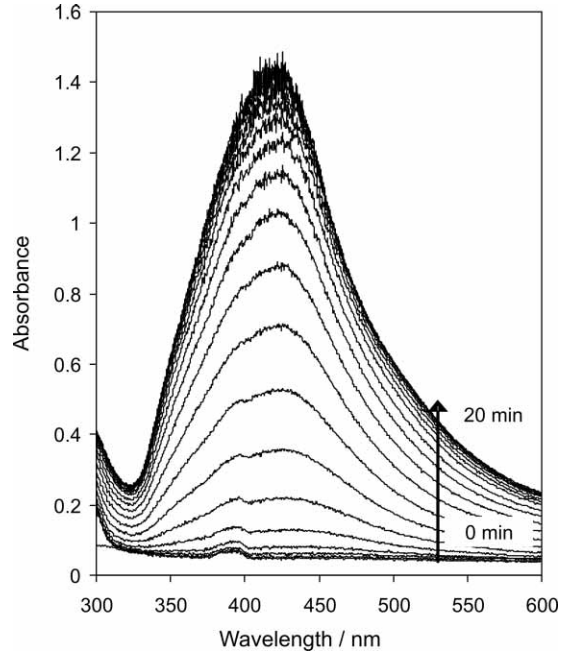

Figure 7. UV-VIS spectra during the synthesis of Ag nanoparticles stabilized by 0.07 g/100 cm^3 PVP solution. The spectra were recorded every minute.

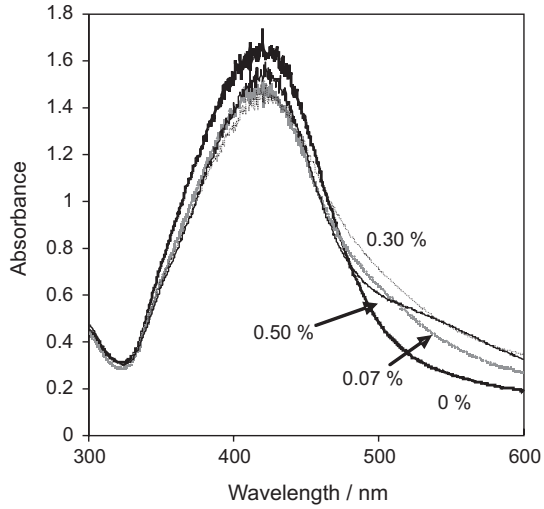

Figure 8. UV-VIS spectra of Ag nanoparticles stabilized at different PVP concentrations after 30 minutes reaction time.

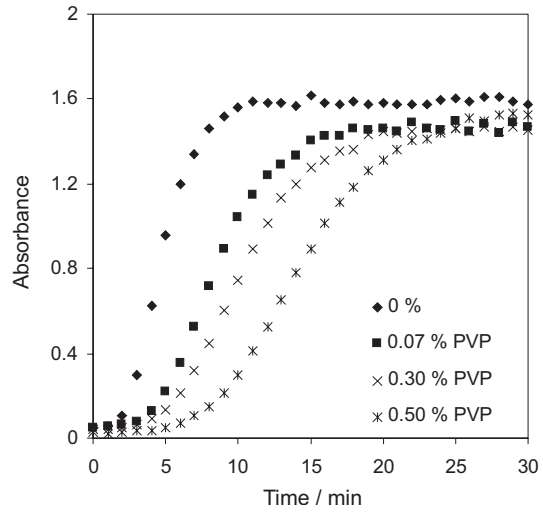

Figure 9. Time course of absorbance at λ = 422 nm: Ag nanoparticles stabilized at various PVP concentrations.

to kinetic and steric inhibition by polymer chains present in the solution, polymer addition slows down both the formation and the growth of particles.

Average particle sizes determined from electron micrographs are listed in Table II. In the absence of polymer, aggregated particles with an average diameter of 9.3 nm are observed (Figure 10a). The sol is quite polydisperse. In the presence of polymer stabilizer, the average particle size decreases (*e.g.*, 0.03 % PVP, d_{TEM} = 2.7 nm) and the distribution is less polydisperse. The size of Ag particle decreases with increasing polymer concentrations; although aggregated particles were also observed at 0.50 % PVP content, the average particle size turned out to be larger than these (5.0 nm). This aggregation could already be predicted from the absorption spectra (Figure 8).

Determination of the Rate of Reduction

The sigmoid course of the kinetic curves in Figure 9, starting with a slow induction period, sharply rising and finally reaching saturation, indicates an autocatalytic reaction.[35,36] If, in our case, the process is indeed autocatalytic, it follows that the function quantitatively describing the progress of reduction, $\ln(a/(1-a))$ (where $a = A_t/A_\infty$, and A_t and A_∞ are maximum absorbances at t and ∞, respectively) changes in a linear fashion in time.[35] Functions $\ln(a/(1-a))$ *vs.* t are represented in Figure 11. Thus, the formation of Ag particles is indeed autocatalytic up to a certain conversion ratio. It can be calculated from the absorbance values that in the absence of polymer the process is autocatalytic up to 92 % conversion whereas at increasing polymer concentrations, autocatalysis ceases at increasingly lower concentrations.

The apparent rate constant of the autocatalytic process (k_a) was determined from the slopes of the $\ln(a/(1-a))$ *vs.* t functions (k_a) (Table II). The value of the rate constant is the highest in the case of the sol without polymer (15.2×10^{-3} s^{-1}), as already shown by the absorbance *vs.* time function. The values of k_a for PVP-containing sols are lower than that for the polymer-free sol. Increasing polymer concentration results in a decrease in the rate constant (8.3×10^{-3} s^{-1} $\rightarrow$ 6.2×10^{-3} s^{-1}).

In order to demonstrate that nucleation and growth can indeed be differentiated on the basis of absorption spectra, the reaction was frozen at certain time points and the

TABLE II. Average particle size and apparent rate constants (k_a, k_1, k_2) of Ag nanoparticle formation at different polymer concentrations

PVP concentration % (ρ)	d_{TEM} nm	$k_a \times 10^3$ s^{-1}	$k_1^{(a)} \times 10^4$ s^{-1}	$k_2^{(b)}$ dm^3 mol^{-1} s^{-1}	$(k_2^{(b)}/k_1^{(a)}) \times 10^{-4}$ dm^3 mol^{-1}
0	9.3±3.9	15.2	2.19	96.99	44
0.07	3.5±1.5	8.3	2.22	50.37	23
0.19	2.9±0.7	8.8	1.74	55.64	32
0.3	2.7±0.8	7.1	1.6	45.86	29
0.5	5.0±2.1	6.2	0.45	41.35	91.8

(a) The apparent rate constant of the nucleation
(b) The apparent rate constant of the paticle growing. Calculation was made from Figure 11 by Refs. 19, 20 and 35.

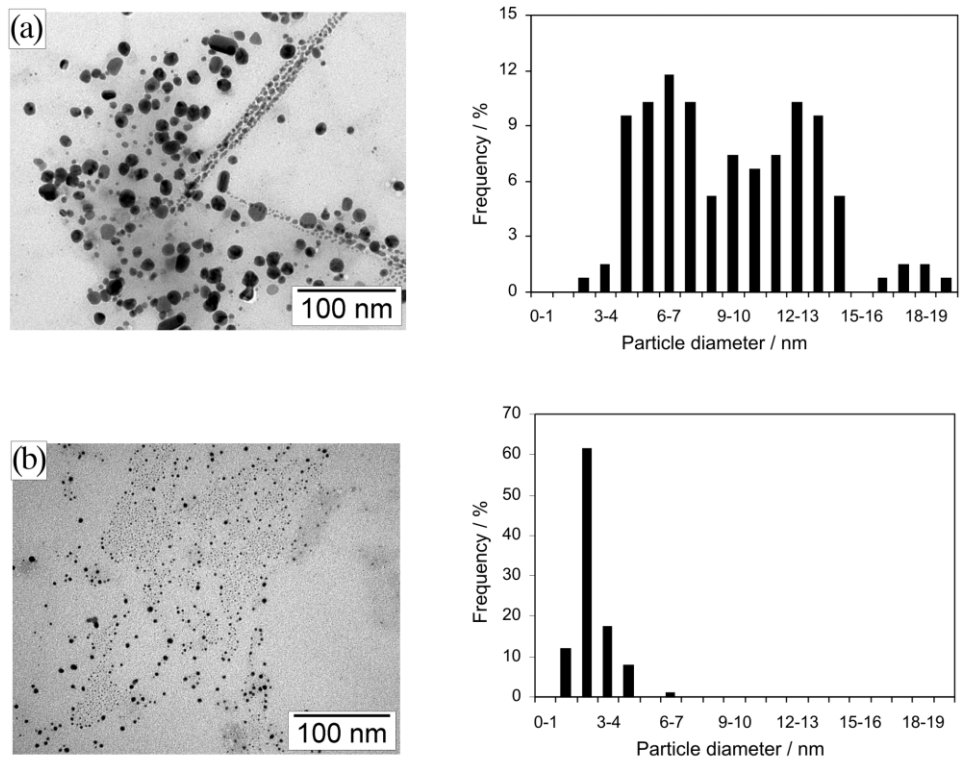

Figure 10. Transmission electron micrograph and particle size distribution of Ag nanoparticles stabilized without polymer (a), with 0.3 g/100 cm^3 PVP (b).

particle size was determined by TEM. Single droplets of sol containing 0.50 % PVP were placed on copper mesh grids covered with Formwar membrane and the samples were then immersed into liquid nitrogen, bringing particle formation and growth to a halt. The samples were subsequently lyophilized. In the nucleation phase, very small particles were observed (d_{TEM} = 2.1 nm after 5 min) at very low densities.

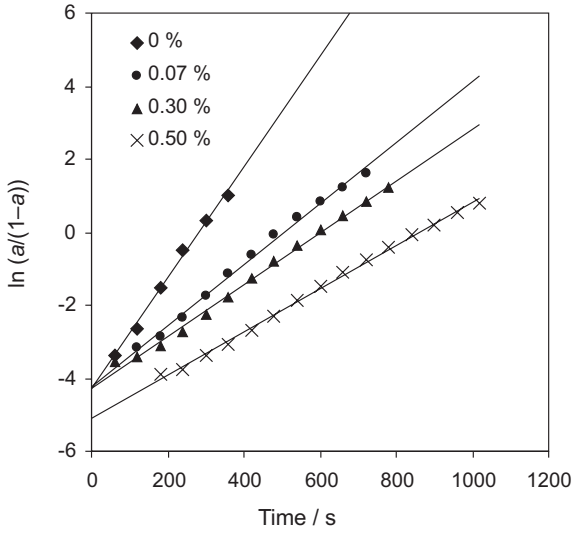

Figure 11. Plots of ln(a/(1–a)) as a function of reaction time.

The 10th minute of the reaction is already at the initial stage of particle growth. At this time, particles with an average diameter of 2.3 nm were present (Figure 12). After 13 min the average particle diameter was 3.1 nm;

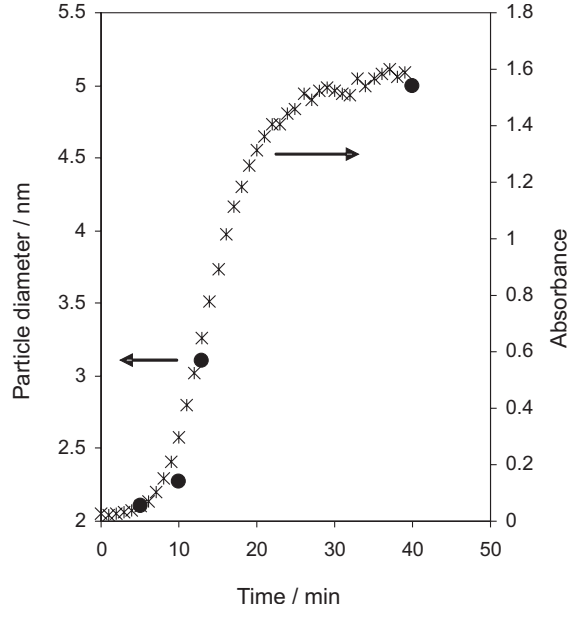

Figure 12. Average particle diameters (•) and absorbance values at λ = 422 nm (*) as a function of reaction time. Ag sol stabilized by 0.50 g/100 cm^3 PVP.

after 40 min particle growth had finished, larger particle aggregates were also present and the average diameter was 5.0 nm. Changes in particle size indicate that the different stages of nucleation and nucleus growth could indeed be differentiated by electron microscopy.

To verify that the process monitored by spectrophotometry was indeed nucleation and nucleus growth, we plotted the kinetic curve of the formation of a sol containing 0.5 g/100 cm^3 PVP and average particle sizes on the same diagram (Figure 12). At first glance, the result is surprising: the increase in particle size corresponds to the increase in absorbance.

CONCLUSIONS

We synthesized palladium and silver nanoparticles by homogeneous nucleation in aqueous medium; the particles were sterically stabilized by PVP. The kinetics of nanoparticle formation was monitored by recording the temporal course of their absorption spectra. We established that nucleation is hindered and the growth rate is slowed by the presence of PVP in the case of both metals. We determined that the formation of silver nanoparticles by hydroquinone reduction is an autocatalytic process: a period of slow, continuous nucleation is followed by rapid, autocatalytic particle growth. The ratio of particle growth/nucleation was used for the estimation of particle size and distribution. The largest particles were formed in sols with the highest growth/nucleation ratios. In these cases, the spectra are broader and a shoulder appears at higher wavelengths, indicating the presence of larger, more polydisperse particles.

REFERENCES

1. J. P. Wilcoxon, R. L. Williamson, and R. Baughman, *J. Chem. Phys.* **98** (1993) 9933–9950.
2. F. Parsapour, D. F. Kelley, S. Craft, and J. P. Wilcoxon, *J. Chem. Phys.* **104** (1996) 4978–4987.
3. N. L. Pocard, D. C. Alsmeyer, R. L. McCreery, T. X. Neenan, and M. R. Callstrom, *J. Am. Chem. Soc.* **114** (1992) 769–771.
4. M. L. Steigerwald and L. E. Brus, *Acc. Chem. Res.* **23** (1990) 183–188.
5. Y. N. Cheomg Chan, R. R. Schrock, and R. E. Cohen, *Chem. Mater.* **4** (1992) 24–27.
6. M. Zhao, L. Sun, and R. M. Crooks, *J. Am. Chem. Soc.* **120** (1998) 4877–4878.
7. J. S. Bradley, *Clusters and Colloids: From Theory to Application*, G. Schmid (Ed.), VCH: New York, 1994, pp. 459–536.
8. L. D. Rampino and F. F. Nord, *J. Am. Chem. Soc.* **63** (1941) 2745–2749.
9. M. Boutonnet, J. Kizling, P. Stenius, and G. Maire, *Colloids Surf.* **5** (1982) 209–225.
10. C. C. Wang, D. H. Chen, and T. C. Huang, *Colloids Surf., A* **189** (2001) 145–154.
11. U. Nickel, A. Castell, K. Pöppl, and S. Schneider, *Langmuir* **16** (2000) 9087–9091.
12. M. Q. Zhao and R. M. Crooks, *Chem. Mater.* **11** (1999) 3379–3385.
13. Y. Nakao and K. Kaeriyama, *J. Colloid Interface Sci.* **110** (1986) 82–87.
14. Z. S. Pillai and P. V. Kamat, *J. Phys. Chem. B* **108** (2004) 945–951.
15. S. M. Heard, F. Grieser, C. G. Barraclough, and J. V. Sanders, *J. Colloid Interface Sci.* **93** (1983) 545–555.
16. W. Hoogsteen and L. G. J. Fokkink, *J. Colloid Interface Sci.* **175** (1995) 12–26.
17. H. Hirai, Y. Nakao, and N. Toshima, *J. Macromol. Sci., Part A* **13** (1979) 727–750.
18. T. Teranishi and M. Miyake, *Chem. Mater.* **10** (1998) 594–600.
19. M. A. Watzky and R. G. Finke, *Chem. Mater.* **9** (1997) 3083–3095.
20. T. Leisner, C. Rosche, S. Wolf, F. Granzer, and L. Woste, *Surf. Rev. Lett.* **3** (1996) 1105–1108.
21. R. Tausch-Treml, A. Henglein, and J. Lilie, *Ber. Bunsen-Ges. Phys. Chem.* **82** (1978) 1335–1343.
22. M. Cai, J. Chen, and J. Zhou, *Appl. Surf. Sci.* **226** (2004) 422–426.
23. S. Ayyappan, R. Srinivasa Gopalan, G. N. Subban, and C. N. R. Rao, *J. Mater. Res.* **12** (1997) 398–401.
24. G. W. Busser, J. G. Ommen, and J. A. Lercher, *J. Phys. Chem. B* **103** (1999) 1651–1659.
25. H. H. Huang, X. P. Ni, G. L. Loy, C. H. Chew, K. L. Tan, F. C. Loh, J. F. Deng, and G. Q. Xu, *Langmuir* **12** (1996) 909–912.
26. K. Esumi, T. Itakura, and K. Torigoe, *Colloids Surf., A* **82** (1994) 111–113.
27. H. S. Kim, J. H. Ryu, B. Jose, B. G. Lee, B. S. Ahn, and Y. S. Kang, *Langmuir* **17** (2001) 5817–5820.
28. D. W. Kim, S. I. Shin, and S. G. Oh, *Adsorption and aggregation of surfactants in solution*, in: K. L. Mittal and D. O. Shah (Eds.), *Surfactant Sciences Series*, Marcel Dekker, New York, Basel, 2003, pp. 255–268.
29. S. A. Vorobyova, N. S. Sobal, and A. I. Lesnikovich, *Colloids Surf., A* **176** (2001) 273–277.
30. N. Shirtcliffe, U. Nickel, and S. Schneider, *J. Colloid Interface Sci.* **211** (1999) 122–129.
31. M. V. Seregina, L. M. Bronstein, O. A. Platonova, D. M. Chernyshov, P. M. Valetsky, J. Hartmann, E. Wenz, and M. Antonietti, *Chem. Mater.* **9** (1997) 923–931.
32. H. H. Ingelsten, R. Bagwe, A. Palmqvist, M. Skoglundh, C. Svanberg, K. Holmberg, and D. O. Shah, *J. Colloid Interface Sci.* **241** (2001) 104–111.
33. L. I. Elding, *Inorg. Chim. Acta* **6** (1972) 647–651.
34. D. N. Furlong, A. Launikonsis, W. H. F. Sasse, and J. W. Sanders, *J. Chem. Soc., Faraday Trans.* **1** (1984) 571–588.
35. K. Esumi, T. Hosoya, A. Yamahira, and K. Torigoe, *J. Colloid Interface Sci.* **226** (2000) 346–352.
36. I. Dékány, R. Krüger-Grasser, and A. Weiss, *Colloid Polym. Sci.* **276** (1998) 570–576.

SAŽETAK

Nastajanje i stabilnost nanočestica plemenitih kovina

Szilvia Papp, Rita Patakfalvi i Imre Dékány

Kinetika homogenih i heterogenih nukleacijskih procesa kovinskih (Ag, Pd) nanočestica istraživana je metodom UV-VIS spektrofotometrije. Nanočestice srebra pripravljene su u vodenoj otopini procesom homogene nukleacije uz uporabu poli(vinilpirolidona) (PVP) i natrijeva citrata kao steričkih stabilizatora. Redukcija je osigurana dodatkom hidrokinona. Prema kinetičkim funkcijama redukcija je autokatalitički proces: sporu, kontinuiranu nukleaciju slijedi brzi, autokatalitički rast. Prisutnost polimera inhibira nukleaciju i smanjuje brzinu rasta čestica. Nastajanje paladijskih nanočestica istraživano je u vodenom mediju putem redukcije hidrazinom, uz uporabu PVP i minerala hektorita kao stabilizatora. Analiziran je utjecaj polimera te koncentracije silikata i iona paladija na brzinu nastajanja čestica. Brzina redukcije smanjivala se s povećanjem udjela stabilizirajućih agensa, dok je rasla s povećanjem koncentracije iona prekursora. Kinetika heterogene nukleacije je određena na osnovi adsorpcije paladija na česticama minerala i viskoznosti disperzije hektorita.